

# Vibration of electro-elastic versus magneto-elastic circular/annular plates using the Chebyshev–Ritz method

C.Y. Dong\*

*Department of Mechanics, School of Science, Beijing Institute of Technology, Beijing 100081, China*

Received 28 November 2007; received in revised form 23 February 2008; accepted 2 March 2008

Handling Editor: L.G. Tham

Available online 14 April 2008

---

## Abstract

The aim of this paper is to analyze three-dimensional free vibration of magneto-elastic/electro-elastic circular/annular plates with different boundary conditions using the Chebyshev–Ritz method, in which a set of duplicate Chebyshev polynomial series multiplied by the boundary function satisfying the boundary conditions are chosen as the trial functions of the displacement components, the electric potential and the magnetic potential. Convergence of the method is checked using various Chebyshev polynomial terms. The effect of geometrical parameters and material properties of magneto-elastic/electro-elastic circular/annular plates on the eigenfrequencies of free vibration is considered.

© 2008 Elsevier Ltd. All rights reserved.

---

## 1. Introduction

Magneto-electro-elastic composite materials can effectively be used to manufacture various sensors and actuators for controlling structural responses, and they also have important applications in the fields of electrics, microwave, supersonics, laser, infrared and so on [1]. Due to their special characteristics, research on the behavior of magneto-electro-elastic structures has been widely carried out. The exact closed-form solution for the simply supported and multilayered plates made of anisotropic piezoelectric and piezomagnetic materials under a static mechanical load has been given by Pan [2]. Free vibration analysis of the simply supported and multilayered plates has been shown by Pan and Heyliger [3]. A finitely long circular cylindrical shell of piezoelectric/piezomagnetic composite under pressuring and temperature change has been solved by Wang and Zhong [4]. The bending analysis of non-homogeneous magneto-electro-elastic-thermo plates has been studied by Chen and Lee [5]. Free vibration study of non-homogeneous transversely isotropic magneto-electro-elastic plates has been done by Chen et al. [6]. Free vibration of an infinite magneto-electro-elastic cylinder has been investigated using semi-analytical finite element method by Buchanan [7]. Free vibration studies of simply supported non-homogeneous functionally graded magneto-electro-elastic finite cylindrical shells has been presented using series solution together with finite element method by Bhangale and

---

\*Corresponding author.

E-mail address: [chunyingdong@yahoo.com](mailto:chunyingdong@yahoo.com)

Ganesan [8]. Free vibrations of clamped–clamped magneto-electro-elastic cylindrical shells have been analyzed using semi-analytical finite element method by Annigeri et al. [9].

The Chebyshev–Ritz method was used to solve the eigenfrequencies of free vibration of various isotropic plates by Zhou et al. [10–12]. The advantage of the Chebyshev–Ritz method is in the fact that the more accurate eigenfrequencies of free vibration of various isotropic plates can be obtained as shown by Zhou et al. [10–12]. It can be expected that the Chebyshev–Ritz method can also be used to obtain the more accurate eigenfrequencies of free vibration of magneto-electro-elastic annular plates with different boundary conditions. Therefore in this paper, three-dimensional (3D) free vibration studies of magneto-elastic/electro-elastic circular/annular plates with various boundary conditions are carried out by the Chebyshev–Ritz method. Convergence of the adopted method is done using various Chebyshev polynomial terms. The effect of geometrical parameters and material properties of the circular/annular plates on the eigenfrequencies of free vibration is considered.

### 2. Basic formulation

One magneto-electro-elastic circular/annular plate with inner radius  $R_0$  and outer radius  $R_1$  and thickness  $h$  is considered. A cylindrical coordinate system  $(r, \theta, z)$  with the origin  $o$  at the circular/annular plate is used to describe the annular plate displacements, i.e. the radial direction displacement  $u$ , the circumferential direction displacement  $v$  and the thickness direction displacement  $w$ , and the electric field  $E_i(i = r, \theta, z)$  and the magnetic field  $H_i(i = r, \theta, z)$ .

Linear elastic strain energy  $V$  for a magneto-electro-elastic circular/annular plate is given as follows:

$$V = \int_0^{2\pi} \int_{R_0}^{R_1} \int_{-h/2}^{h/2} \left( \frac{1}{2} \mathbf{S}^T \mathbf{C} \mathbf{S} - \frac{1}{2} \mathbf{E}^T \boldsymbol{\varepsilon} \mathbf{E} - \frac{1}{2} \mathbf{H}^T \boldsymbol{\mu} \mathbf{H} - \mathbf{S}^T \mathbf{e} \mathbf{E} - \mathbf{S}^T \mathbf{q} \mathbf{H} - \mathbf{E}^T \mathbf{m} \mathbf{H} \right) r \, dz \, dr \, d\theta \tag{1}$$

where

$$\begin{aligned} \mathbf{S} &= [S_{rr} \quad S_{\theta\theta} \quad S_{zz} \quad S_{\theta z} \quad S_{rz} \quad S_{r\theta}]^T, \quad \mathbf{E} = [E_r \quad E_\theta \quad E_z]^T, \quad \mathbf{H} = [H_r \quad H_\theta \quad H_z]^T, \\ \mathbf{C} &= \begin{bmatrix} C_{11} & C_{12} & C_{13} & 0 & 0 & 0 \\ C_{12} & C_{22} & C_{13} & 0 & 0 & 0 \\ C_{13} & C_{13} & C_{13} & 0 & 0 & 0 \\ 0 & 0 & 0 & C_{44} & 0 & 0 \\ 0 & 0 & 0 & 0 & C_{44} & 0 \\ 0 & 0 & 0 & 0 & 0 & C_{66} \end{bmatrix}, \quad \boldsymbol{\varepsilon} = \begin{bmatrix} \varepsilon_{11} & 0 & 0 \\ 0 & \varepsilon_{11} & 0 \\ 0 & 0 & \varepsilon_{33} \end{bmatrix}, \quad \boldsymbol{\mu} = \begin{bmatrix} \mu_{11} & 0 & 0 \\ 0 & \mu_{11} & 0 \\ 0 & 0 & \mu_{33} \end{bmatrix}, \\ \mathbf{e} &= \begin{bmatrix} 0 & 0 & e_{31} \\ 0 & 0 & e_{31} \\ 0 & 0 & e_{33} \\ 0 & e_{15} & 0 \\ e_{15} & 0 & 0 \\ 0 & 0 & 0 \end{bmatrix}, \quad \mathbf{q} = \begin{bmatrix} 0 & 0 & q_{31} \\ 0 & 0 & q_{31} \\ 0 & 0 & q_{33} \\ 0 & q_{15} & 0 \\ q_{15} & 0 & 0 \\ 0 & 0 & 0 \end{bmatrix}, \quad \boldsymbol{\mu} = \begin{bmatrix} m_{11} & 0 & 0 \\ 0 & m_{11} & 0 \\ 0 & 0 & m_{33} \end{bmatrix}, \\ S_{rr} &= \frac{\partial u}{\partial r}, \quad S_{\theta\theta} = \frac{1}{r} \left( \frac{\partial v}{\partial r} + u \right), \quad S_{zz} = \frac{\partial w}{\partial z}, \quad S_{r\theta} = \frac{1}{r} \frac{\partial u}{\partial \theta} + \frac{\partial v}{\partial r} - \frac{v}{r}, \quad S_{rz} = \frac{\partial w}{\partial r} + \frac{\partial u}{\partial z}, \\ S_{\theta z} &= \frac{\partial v}{\partial z} + \frac{1}{r} \frac{\partial w}{\partial \theta}, \quad E_r = -\frac{\partial \phi}{\partial r}, \quad E_\theta = -\frac{1}{r} \frac{\partial \phi}{\partial \theta}, \quad E_z = -\frac{\partial \phi}{\partial z}, \quad H_r = -\frac{\partial \psi}{\partial r}, \\ H_\theta &= -\frac{1}{r} \frac{\partial \psi}{\partial \theta}, \quad H_z = -\frac{\partial \psi}{\partial z} \end{aligned} \tag{2}$$

where  $\varphi$  and  $\psi$  are, respectively, the electric potential and the magnetic potential;  $C_{ij}$ ,  $\epsilon_{ij}$  and  $\mu_{ij}$  are the elastic, dielectric and magnetic permeability coefficients, respectively;  $e_{ij}$ ,  $q_{ij}$  and  $m_{ij}$  are the piezoelectric, piezomagnetic and magnetolectric material coefficients, respectively.

The kinetic energy  $T$  of the circular/annular plate can be given as

$$T = \frac{\rho}{2} \int_0^{2\pi} \int_{R_0}^{R_1} \int_{-h/2}^{h/2} \left[ \left( \frac{\partial u}{\partial t} \right)^2 + \left( \frac{\partial v}{\partial t} \right)^2 + \left( \frac{\partial w}{\partial t} \right)^2 \right] r \, dz \, dr \, d\theta \tag{3}$$

where  $\rho$  is the mass density per unit volume of the circular/annular plate.

In numerical implementation, some dimensionless parameters are introduced [11], i.e.

$$\bar{r} = \frac{2r}{R} - \delta, \quad \bar{\theta} = \theta, \quad \bar{z} = \frac{2z}{h} \tag{4}$$

where

$$\bar{R} = R_1 - R_0, \quad \delta = \frac{R_1 + R_0}{R_1 - R_0}$$

In the situation of free vibration, the displacement components and the electric potential and the magnetic potential of the annular plate can be expressed into the following forms:

$$\begin{aligned} u(r, \theta, z, t) &= U(\bar{r}, \bar{\theta}, \bar{z}) e^{i\omega t}, & v(r, \theta, z, t) &= \hat{V}(\bar{r}, \bar{\theta}, \bar{z}) e^{i\omega t}, & w(r, \theta, z, t) &= W(\bar{r}, \bar{\theta}, \bar{z}) e^{i\omega t}, \\ \varphi(r, \theta, z, t) &= \Phi(\bar{r}, \bar{\theta}, \bar{z}) e^{i\omega t}, & \psi(r, \theta, z, t) &= \Psi(\bar{r}, \bar{\theta}, \bar{z}) e^{i\omega t} \end{aligned} \tag{5}$$

where  $\omega$  is the eigenfrequency of the circular/annular plate and  $i = \sqrt{-1}$ .

Considering the circumferential symmetry of the circular/annular plate about the coordinate  $\theta$ , the displacement amplitude functions, electric potential amplitude functions and magnetic potential amplitude functions can be expressed as trigonometric functions in the circumferential direction as

$$\begin{aligned} U(\bar{r}, \bar{\theta}, \bar{z}) &= \bar{U}(\bar{r}, \bar{z}) \cos(s\bar{\theta}) \\ \hat{V}(\bar{r}, \bar{\theta}, \bar{z}) &= \bar{V}(\bar{r}, \bar{z}) \sin(s\bar{\theta}) \\ W(\bar{r}, \bar{\theta}, \bar{z}) &= \bar{W}(\bar{r}, \bar{z}) \cos(s\bar{\theta}) \\ \Phi(\bar{r}, \bar{\theta}, \bar{z}) &= \bar{\Phi}(\bar{r}, \bar{z}) \cos(s\bar{\theta}) \\ \Psi(\bar{r}, \bar{\theta}, \bar{z}) &= \bar{\Psi}(\bar{r}, \bar{z}) \cos(s\bar{\theta}) \end{aligned} \tag{6}$$

where  $s = 0, 1, \dots, \infty$ . As mentioned by Zhou et al. [11],  $s = 0$  means the axisymmetric vibration, i.e.

$$\begin{aligned} U(\bar{r}, \bar{\theta}, \bar{z}) &= \bar{U}(\bar{r}, \bar{z}), & \hat{V}(\bar{r}, \bar{\theta}, \bar{z}) &= 0, & W(\bar{r}, \bar{\theta}, \bar{z}) &= \bar{W}(\bar{r}, \bar{z}), & \Phi(\bar{r}, \bar{\theta}, \bar{z}) &= \bar{\Phi}(\bar{r}, \bar{z}), \\ \Psi(\bar{r}, \bar{\theta}, \bar{z}) &= \bar{\Psi}(\bar{r}, \bar{z}). \end{aligned}$$

Rotating the symmetry axes by  $\pi/2$ , another set of free vibration modes can be obtained, corresponding to an interchange of  $\cos(s\bar{\theta})$  and  $\sin(s\bar{\theta})$  in Eq. (6). For this case,  $s = 0$  means the torsional vibration, i.e.  $U(\bar{r}, \bar{\theta}, \bar{z}) = 0$ ,  $\hat{V}(\bar{r}, \bar{\theta}, \bar{z}) = \bar{V}(\bar{r}, \bar{z})$ ,  $W(\bar{r}, \bar{\theta}, \bar{z}) = 0$ ,  $\Phi(\bar{r}, \bar{\theta}, \bar{z}) = 0$ ,  $\Psi(\bar{r}, \bar{\theta}, \bar{z}) = 0$ .

Based on Eqs. (4)–(6), Eqs. (1) and (3) can be changed into the following forms:

$$V = \frac{h}{2} \int_{-1}^1 \int_{-1}^1 \left\{ \frac{1}{2} \begin{bmatrix} \bar{S}_{rr} & \bar{S}_{\theta\theta} & \bar{S}_{zz} & \bar{S}_{rz} \end{bmatrix} \begin{bmatrix} C_{11} & C_{12} & C_{13} & 0 \\ C_{12} & C_{11} & C_{13} & 0 \\ C_{13} & C_{13} & C_{33} & 0 \\ 0 & 0 & 0 & C_{44} \end{bmatrix} \begin{Bmatrix} \bar{S}_{rr} \\ \bar{S}_{\theta\theta} \\ \bar{S}_{zz} \\ \bar{S}_{rz} \end{Bmatrix} \right\} \Gamma_1$$

$$\begin{aligned}
 & + \frac{1}{2} \begin{bmatrix} \bar{S}_{\theta z} & \bar{S}_{r\theta} \end{bmatrix} \begin{bmatrix} C_{44} & 0 \\ 0 & C_{66} \end{bmatrix} \begin{Bmatrix} \bar{S}_{\theta z} \\ \bar{S}_{r\theta} \end{Bmatrix} \Gamma_2 - \frac{1}{2} \begin{bmatrix} \bar{E}_r & \bar{E}_z \end{bmatrix} \begin{bmatrix} \varepsilon_{11} & 0 \\ 0 & \varepsilon_{33} \end{bmatrix} \begin{Bmatrix} \bar{E}_r \\ \bar{E}_z \end{Bmatrix} \Gamma_1 \\
 & - \frac{1}{2} \varepsilon_{11} \bar{E}_\theta^2 \Gamma_2 - \frac{1}{2} \begin{bmatrix} \bar{H}_r & \bar{H}_z \end{bmatrix} \begin{bmatrix} \mu_{11} & 0 \\ 0 & \mu_{33} \end{bmatrix} \begin{Bmatrix} \bar{H}_r \\ \bar{H}_z \end{Bmatrix} \Gamma_1 - \frac{1}{2} \mu_{11} \bar{H}_\theta^2 \Gamma_2 \\
 & - \begin{bmatrix} \bar{S}_{rr} & \bar{S}_{\theta\theta} & \bar{S}_{zz} & \bar{S}_{rz} \end{bmatrix} \begin{bmatrix} 0 & e_{31} \\ 0 & e_{31} \\ 0 & e_{33} \\ e_{15} & 0 \end{bmatrix} \begin{Bmatrix} \bar{E}_r \\ \bar{E}_z \end{Bmatrix} \Gamma_1 - e_{15} \bar{S}_{\theta z} \bar{E}_\theta \Gamma_2 \\
 & - \begin{bmatrix} \bar{S}_{rr} & \bar{S}_{\theta\theta} & \bar{S}_{zz} & \bar{S}_{rz} \end{bmatrix} \begin{bmatrix} 0 & q_{31} \\ 0 & q_{31} \\ 0 & q_{33} \\ q_{15} & 0 \end{bmatrix} \begin{Bmatrix} \bar{H}_r \\ \bar{H}_z \end{Bmatrix} \Gamma_1 - q_{15} \bar{S}_{\theta z} \bar{H}_\theta \Gamma_2 \\
 & - \left. \begin{bmatrix} \bar{E}_r & \bar{E}_z \end{bmatrix} \begin{bmatrix} m_{11} & 0 \\ 0 & m_{33} \end{bmatrix} \begin{Bmatrix} \bar{H}_r \\ \bar{H}_z \end{Bmatrix} \Gamma_1 - m_{11} \bar{E}_\theta \bar{H}_\theta \Gamma_2 \right\} (\bar{r} + \delta) d\bar{z} d\bar{r} \tag{7}
 \end{aligned}$$

and

$$T = \frac{\rho \bar{R}^2 h}{16} \omega^2 \int_{-1}^1 \int_{-1}^1 (\Gamma_1 \bar{U}^2 + \Gamma_2 \bar{V}^2 + \Gamma_3 \bar{W}^2) (\bar{r} + \delta) d\bar{z} d\bar{r} \tag{8}$$

where

$$\begin{aligned}
 \bar{S}_{rr} &= \frac{\partial \bar{u}}{\partial \bar{r}}, & \bar{S}_{\theta\theta} &= \frac{1}{\bar{r} + \delta} (\bar{u} + s\bar{v}), & \bar{S}_{zz} &= \frac{\partial \bar{w}}{\partial \bar{z}}, & \bar{S}_{r\theta} &= -\frac{\bar{v} + s\bar{u}}{\bar{r} + \delta} + \frac{\partial \bar{v}}{\partial \bar{r}}, & \bar{S}_{rz} &= \frac{\partial \bar{w}}{\partial \bar{r}} + \frac{\partial \bar{u}}{\partial \bar{z}}, \\
 \bar{S}_{\theta z} &= \frac{\partial \bar{v}}{\partial \bar{z}} - \frac{s\bar{w}}{\bar{r} + \delta}, & \bar{E}_r &= -\frac{\partial \bar{\phi}}{\partial \bar{r}}, & \bar{E}_\theta &= \frac{s\bar{\phi}}{\bar{r} + \delta}, \\
 \bar{E}_z &= -\frac{\partial \bar{\phi}}{\partial \bar{z}}, & \bar{H}_r &= -\frac{\partial \bar{\psi}}{\partial \bar{r}}, & \bar{H}_\theta &= \frac{s\bar{\psi}}{\bar{r} + \delta}, & \bar{H}_z &= -\frac{\partial \bar{\psi}}{\partial \bar{z}}, & \bar{\gamma} &= h/\bar{R}
 \end{aligned}$$

$$\begin{aligned}
 \Gamma_1 &= \int_0^{2\pi} \cos^2(s\theta) d\theta = \begin{cases} 2\pi & (s = 0) \\ \pi & (s > 0) \end{cases} \\
 \Gamma_2 &= \int_0^{2\pi} \sin^2(s\theta) d\theta = \begin{cases} 0 & (s = 0) \\ \pi & (s > 0) \end{cases} \tag{9}
 \end{aligned}$$

Each of the displacement amplitude functions, the electric potential and the magnetic potential can be written as double series of Chebyshev polynomials multiplied by boundary functions, i.e.

$$\begin{aligned}
 \bar{U}(\bar{r}, \bar{z}) &= F_u^0(\bar{r}) F_u^1(\bar{r}) \sum_{i=1}^I \sum_{j=1}^J A_{ij} P_i(\bar{r}) P_j(\bar{z}) \\
 \bar{V}(\bar{r}, \bar{z}) &= F_v^0(\bar{r}) F_v^1(\bar{r}) \sum_{k=1}^K \sum_{l=1}^L B_{kl} P_k(\bar{r}) P_l(\bar{z})
 \end{aligned}$$

$$\begin{aligned} \overline{W}(\bar{r}, \bar{z}) &= F_w^0(\bar{r})F_w^1(\bar{r}) \sum_{m=1}^M \sum_{n=1}^N C_{mn}P_m(\bar{r})P_n(\bar{z}) \\ \overline{\Phi}(\bar{r}, \bar{z}) &= F_\varphi^0(\bar{r})F_\varphi^1(\bar{r}) \sum_{o=1}^O \sum_{p=1}^P D_{op}P_o(\bar{r})P_p(\bar{z}) \\ \overline{\Psi}(\bar{r}, \bar{z}) &= F_\psi^0(\bar{r})F_\psi^1(\bar{r}) \sum_{q=1}^Q \sum_{h=1}^H E_{qh}P_q(\bar{r})P_h(\bar{z}) \end{aligned} \tag{10}$$

where  $I, J, K, L, M, N, O, P, Q$  and  $H$  are the truncation orders of the Chebyshev polynomial series;  $A_{ij}, B_{kl}, C_{mn}, D_{op}$  and  $E_{qh}$  are the coefficients to be determined;  $P_i(\chi)$  ( $i = 1, 2, \dots; \chi = \bar{r}, \bar{z}$ ) is the one-dimensional (1D)  $i$ th Chebyshev polynomial, i.e.

$$P_i(\chi) = \cos[(i - 1) \arccos(\chi)], \quad i = 1, 2, 3, \dots \tag{11}$$

The choice of the boundary functions  $F_u^i, F_v^i, F_w^i, F_\varphi^i, F_\psi^i$  ( $i = 0, 1$ ) is to make the displacement components ( $u, v, w$ ), the electric potential  $\varphi$  and the magnetic potential  $\psi$  to satisfy the inner and outer geometric boundary conditions, the electric potential and the magnetic potential boundary conditions of the circular/annular plate, respectively.

The energy functional  $\Pi$  of the circular/annular plate is as follows:

$$\Pi = V - T \tag{12}$$

Based on Ritz method, we have

$$\frac{\partial \Pi}{\partial A_{ij}} = 0, \quad \frac{\partial \Pi}{\partial B_{kl}} = 0, \quad \frac{\partial \Pi}{\partial C_{mn}} = 0, \quad \frac{\partial \Pi}{\partial D_{op}} = 0, \quad \frac{\partial \Pi}{\partial E_{qh}} = 0 \tag{13}$$

Thus, the eigenfrequency equation of the circular/annular plate can be obtained as follows:

$$\left( \begin{bmatrix} \mathbf{K}_{uu} & \mathbf{K}_{uv} & \mathbf{K}_{uw} & \mathbf{K}_{u\varphi} & \mathbf{K}_{u\psi} \\ \mathbf{K}_{uv}^T & \mathbf{K}_{vv} & \mathbf{K}_{vw} & \mathbf{K}_{v\varphi} & \mathbf{K}_{v\psi} \\ \mathbf{K}_{uw}^T & \mathbf{K}_{vw}^T & \mathbf{K}_{ww} & \mathbf{K}_{w\varphi} & \mathbf{K}_{w\psi} \\ \mathbf{K}_{u\varphi}^T & \mathbf{K}_{v\varphi}^T & \mathbf{K}_{w\varphi}^T & \mathbf{K}_{\varphi\varphi} & \mathbf{K}_{\varphi\psi} \\ \mathbf{K}_{u\psi}^T & \mathbf{K}_{v\psi}^T & \mathbf{K}_{w\psi}^T & \mathbf{K}_{\varphi\psi}^T & \mathbf{K}_{\psi\psi} \end{bmatrix} - \overline{\Omega}^2 \begin{bmatrix} \mathbf{M}_{uu} & \mathbf{0} & \mathbf{0} & \mathbf{0} & \mathbf{0} \\ \mathbf{0} & \mathbf{M}_{vv} & \mathbf{0} & \mathbf{0} & \mathbf{0} \\ \mathbf{0} & \mathbf{0} & \mathbf{M}_{ww} & \mathbf{0} & \mathbf{0} \\ \mathbf{0} & \mathbf{0} & \mathbf{0} & \mathbf{0} & \mathbf{0} \\ \mathbf{0} & \mathbf{0} & \mathbf{0} & \mathbf{0} & \mathbf{0} \end{bmatrix} \right) \begin{Bmatrix} \mathbf{A} \\ \mathbf{B} \\ \mathbf{C} \\ \mathbf{D} \\ \mathbf{E} \end{Bmatrix} = \begin{Bmatrix} \mathbf{0} \\ \mathbf{0} \\ \mathbf{0} \\ \mathbf{0} \\ \mathbf{0} \end{Bmatrix} \tag{14}$$

where  $\overline{\Omega} = \overline{R}\omega\sqrt{\rho}$ ;  $\mathbf{K}_{ij}(i, j = u, v, w, \varphi, \psi)$  and  $\mathbf{M}_{ij}(i, j = u, v, w)$  are, respectively, the coefficient matrices related to the column vectors  $\mathbf{A}, \mathbf{B}, \mathbf{C}, \mathbf{D}$  and  $\mathbf{E}$  which are as follows:

$$\begin{aligned} \mathbf{A} &= [A_{11} \quad \dots \quad A_{1J} \quad A_{21} \quad \dots \quad A_{2J} \quad \dots \quad A_{I1} \quad \dots \quad A_{IJ}]^T, \\ \mathbf{B} &= [B_{11} \quad \dots \quad B_{1L} \quad B_{21} \quad \dots \quad B_{2L} \quad \dots \quad B_{K1} \quad \dots \quad B_{KL}]^T, \\ \mathbf{C} &= [C_{11} \quad \dots \quad C_{1N} \quad C_{21} \quad \dots \quad C_{2N} \quad \dots \quad C_{M1} \quad \dots \quad C_{MN}]^T, \\ \mathbf{D} &= [D_{11} \quad \dots \quad D_{1P} \quad D_{21} \quad \dots \quad D_{2P} \quad \dots \quad D_{O1} \quad \dots \quad D_{OP}]^T, \\ \mathbf{E} &= [E_{11} \quad \dots \quad E_{1H} \quad E_{21} \quad \dots \quad E_{2H} \quad \dots \quad E_{Q1} \quad \dots \quad E_{QH}]^T \end{aligned} \tag{15}$$

The detailed expressions of the matrices  $\mathbf{K}_{ij}(i, j = u, v, w, \varphi, \psi)$  and  $\mathbf{M}_{ij}(i, j = u, v, w)$  are omitted for simplicity.

In Eq. (14), the electric potential and magnetic potential terms are eliminated by condensation techniques. Thus, the resulting matrix for solving the eigenvalues is obtained as follows:

$$\left( \begin{bmatrix} \tilde{\mathbf{K}}_{uu} & \tilde{\mathbf{K}}_{uv} & \tilde{\mathbf{K}}_{uw} \\ \tilde{\mathbf{K}}_{uv}^T & \tilde{\mathbf{K}}_{vv} & \tilde{\mathbf{K}}_{vw} \\ \tilde{\mathbf{K}}_{uw}^T & \tilde{\mathbf{K}}_{vw}^T & \tilde{\mathbf{K}}_{ww} \end{bmatrix} - \bar{\Omega}^2 \begin{bmatrix} \mathbf{M}_{uu} & \mathbf{0} & \mathbf{0} \\ \mathbf{0} & \mathbf{M}_{vv} & \mathbf{0} \\ \mathbf{0} & \mathbf{0} & \mathbf{M}_{ww} \end{bmatrix} \right) \begin{Bmatrix} \mathbf{A} \\ \mathbf{B} \\ \mathbf{C} \end{Bmatrix} = \begin{Bmatrix} \mathbf{0} \\ \mathbf{0} \\ \mathbf{0} \end{Bmatrix} \quad (16)$$

where

$$\begin{bmatrix} \tilde{\mathbf{K}}_{uu} & \tilde{\mathbf{K}}_{uv} & \tilde{\mathbf{K}}_{uw} \\ \tilde{\mathbf{K}}_{uv}^T & \tilde{\mathbf{K}}_{vv} & \tilde{\mathbf{K}}_{vw} \\ \tilde{\mathbf{K}}_{uw}^T & \tilde{\mathbf{K}}_{vw}^T & \tilde{\mathbf{K}}_{ww} \end{bmatrix} = \begin{bmatrix} \mathbf{K}_{uu} & \mathbf{K}_{uv} & \mathbf{K}_{uw} \\ \mathbf{K}_{uv}^T & \mathbf{K}_{vv} & \mathbf{K}_{vw} \\ \mathbf{K}_{uw}^T & \mathbf{K}_{vw}^T & \mathbf{K}_{ww} \end{bmatrix} - \begin{bmatrix} \mathbf{K}_{u\varphi} & \mathbf{K}_{u\psi} \\ \mathbf{K}_{v\varphi} & \mathbf{K}_{v\psi} \\ \mathbf{K}_{w\varphi} & \mathbf{K}_{w\psi} \end{bmatrix} \begin{bmatrix} \mathbf{K}_{\varphi\varphi} & \mathbf{K}_{\varphi\psi} \\ \mathbf{K}_{\varphi\psi}^T & \mathbf{K}_{\psi\psi} \end{bmatrix}^T \begin{bmatrix} \mathbf{K}_{u\varphi}^T & \mathbf{K}_{v\varphi}^T & \mathbf{K}_{w\varphi}^T \\ \mathbf{K}_{u\psi}^T & \mathbf{K}_{v\psi}^T & \mathbf{K}_{w\psi}^T \end{bmatrix} \quad (17)$$

From Eq. (16), the eigenvalues  $\bar{\Omega}$  and the corresponding modes shapes can be obtained using numerical methods such as the QR algorithm [13].

### 3. Numerical examples

#### 3.1. Piezoelectric circular/annular plate

A piezoelectric circular/annular plate is studied herein. The material parameters are as follows:

$$\begin{aligned} C_{11} &= 13.9 \times 10^{10} \text{ Pa}, & C_{12} &= 7.78 \times 10^{10} \text{ Pa}, & C_{13} &= 7.43 \times 10^{10} \text{ Pa}, & C_{33} &= 11.5 \times 10^{10} \text{ Pa}, \\ C_{44} &= 2.56 \times 10^{10} \text{ Pa}, & e_{15} &= 12.7 \text{ C/m}^2, & e_{31} &= -5.2 \text{ C/m}^2, & e_{33} &= 15.1 \text{ C/m}^2, \\ \varepsilon_{11} &= 6.46 \times 10^{-9} \text{ F/m}, & \varepsilon_{33} &= 5.62 \times 10^{-9} \text{ F/m}. \end{aligned}$$

The ratio of the inner radius  $R_0$  and outer radius  $R_1$  of the circular/annular plate is  $R_1/R_0 = 2$ , its thickness is  $h/R_1 = 0.1$ . For comparison, the non-dimensional free vibration first frequency,  $\Omega = \omega h \sqrt{\rho/C_{11}}$ , for wave number  $s = 1, 2, 3$  for piezoelectric circular/annular plate with boundary condition, i.e.  $v = 0, w = 0, \varphi = 0$  along inner and outer circumferential boundaries is calculated and shown in Table 1. Note that Chebyshev polynomial terms are taken as  $I = K = N = O = Q = 10, J = L = N = P = H = 10$  in calculation. One can find that excellent agreement between the present results and those from Wang et al. [14] has been observed.

#### 3.2. Magneto-elastic/electro-elastic annular plates

Magneto-elastic/electro-elastic annular plates with inner radius  $R_0$  and outer radius  $R_1$  as well as thickness  $h$  ( $R_1/R_0 = 2.5, h/R_1 = 0.5$ ) are studied here. The first eight free vibration frequencies will be calculated and compared for plates of  $\text{BaTiO}_3$  and  $\text{CoFe}_2\text{O}_4$ , respectively. The material data are shown in Table 2 [7].

Table 1  
The non-dimensional first frequency of circular annular plate

Methods	$s = 1$	$s = 2$	$s = 3$
Present	0.1050	0.1177	0.1386
Wang et al. [14]	0.1023	0.1152	0.1362

Table 2  
Material properties for piezoelectric barium titanate and magnetostrictive cobalt iron oxide [7]

Material coefficient	BaTiO <sub>3</sub>	CoFe <sub>2</sub> O <sub>4</sub>
$C_{11}$ (10 <sup>9</sup> ) (N/m <sup>2</sup> )	166	286
$C_{33}$	162	269.5
$C_{12}$	77	173
$C_{13}$	78	170
$C_{44}$	43	45.3
$C_{66}$	44.5	56.5
$e_{15}$ (C/m <sup>2</sup> )	11.6	0
$e_{31}$	-4.4	0
$e_{33}$	18.6	0
$\epsilon_{11}$ (10 <sup>-9</sup> ) (C/V m)	11.2	0.08
$\epsilon_{33}$	12.6	0.093
$q_{15}$ (N/A m)	0	550
$q_{31}$	0	580.3
$q_{33}$	0	699.7
$\mu_{11}$ (10 <sup>-6</sup> ) (N s <sup>2</sup> /C <sup>2</sup> )	5.0	-590
$\mu_{33}$	10.0	157
$m_{11}$ (10 <sup>-9</sup> ) (N s <sup>2</sup> /V C)	0	0
$m_{33}$	0	0

Table 3  
Convergence of the first eight eigenfrequency parameters for the clamped–clamped annular BaTiO<sub>3</sub>/CoFe<sub>2</sub>O<sub>4</sub> plates

$s$	$I \times J$	BaTiO <sub>3</sub>								CoFe <sub>2</sub> O <sub>4</sub>							
		$\Omega_1$	$\Omega_2$	$\Omega_3$	$\Omega_4$	$\Omega_5$	$\Omega_6$	$\Omega_7$	$\Omega_8$	$\Omega_1$	$\Omega_2$	$\Omega_3$	$\Omega_4$	$\Omega_5$	$\Omega_6$	$\Omega_7$	$\Omega_8$
0	9 × 4	2.866	5.524	5.640	7.076	7.277	8.210	8.968	9.871	2.914	5.693	6.314	7.634	8.380	8.990	9.326	10.63
	20 × 12	2.837	5.492	5.587	6.926	7.191	7.828	8.845	9.589	2.859	5.628	6.255	7.453	8.357	8.684	8.817	10.47
	26 × 22	2.833	5.456	5.582	6.912	7.183	7.801	8.796	9.563	2.858	5.627	6.253	7.451	8.356	8.683	8.816	10.47
1	20 × 12	2.926	3.547	5.182	5.523	5.738	6.629	6.885	7.218	2.922	3.916	5.424	5.723	6.166	7.231	7.306	8.054
	24 × 20	2.886	3.545	5.172	5.515	5.625	6.622	6.839	7.154	2.921	3.916	5.424	5.722	6.165	7.230	7.304	8.054
	26 × 22	2.884	3.545	5.171	5.514	5.580	6.619	6.815	7.158	2.921	3.916	5.424	5.722	6.164	7.230	7.304	8.054
2	9 × 4	3.309	4.186	5.549	5.669	6.329	7.004	7.142	7.823	3.197	4.632	5.853	6.144	6.180	7.297	7.557	8.340
	20 × 12	3.153	4.159	5.507	5.596	6.056	6.825	6.867	7.281	3.149	4.622	5.812	6.110	6.121	7.230	7.485	7.973
	24 × 20	3.102	4.153	5.503	5.556	5.967	6.789	6.827	7.233	3.149	4.622	5.811	6.109	6.120	7.229	7.484	7.973
	26 × 22	3.101	4.152	5.502	5.555	5.914	6.769	6.828	7.231	3.149	4.622	5.811	6.109	6.120	7.229	7.484	7.973
3	9 × 4	3.770	4.890	5.768	6.171	6.873	7.235	7.440	8.110	3.607	5.390	6.251	6.321	6.829	7.481	7.830	8.549
	20 × 12	3.566	4.842	5.726	6.037	6.594	6.968	7.066	7.559	3.558	5.370	6.186	6.307	6.729	7.437	7.750	8.182
	24 × 20	3.501	4.833	5.720	5.981	6.489	6.952	6.993	7.525	3.558	5.370	6.186	6.306	6.728	7.437	7.750	8.181
	26 × 22	3.503	4.832	5.719	5.961	6.437	6.944	6.996	7.505	3.558	5.370	6.186	6.306	6.728	7.437	7.749	8.181

In calculation process, Chebyshev polynomial terms are taken as  $I = K = N = O = Q, J = L = N = P = H$  for convenience. The non-dimensional free vibration frequencies for wave number  $s = 0, 1, 2, 3$  for plates of BaTiO<sub>3</sub> and CoFe<sub>2</sub>O<sub>4</sub>, i.e.  $\Omega = \sqrt{\bar{\Omega}/C_{44}}$ , with different boundary conditions are, respectively, listed in Tables 3–5. It should be noted that the symbol “clamped–free” denotes an annular with the inner and outer circumferences having fixed and free boundary conditions, respectively. Similarly, the symbol “clamped–clamped” (“free–clamped”) denotes an annular with the inner and outer circumferences having fixed and fixed (free and clamped) boundary conditions, respectively. One can find that with the increase of Chebyshev polynomial terms the convergent solution can be obtained. Relatively, for various boundary conditions, the

Table 4  
Convergence of the first eight eigenfrequency parameters for the clamped–free annular BaTiO<sub>3</sub>/CoFe<sub>2</sub>O<sub>4</sub> plates

<i>s</i>	<i>I</i> × <i>J</i>	BaTiO <sub>3</sub>								CoFe <sub>2</sub> O <sub>4</sub>							
		Ω <sub>1</sub>	Ω <sub>2</sub>	Ω <sub>3</sub>	Ω <sub>4</sub>	Ω <sub>5</sub>	Ω <sub>6</sub>	Ω <sub>7</sub>	Ω <sub>8</sub>	Ω <sub>1</sub>	Ω <sub>2</sub>	Ω <sub>3</sub>	Ω <sub>4</sub>	Ω <sub>5</sub>	Ω <sub>6</sub>	Ω <sub>7</sub>	Ω <sub>8</sub>
0	9 × 4	1.061	2.855	3.927	6.082	6.519	7.141	7.434	8.356	0.980	3.080	3.275	5.491	6.513	6.983	7.095	9.437
	24 × 20	1.036	2.839	3.741	5.986	6.295	6.999	7.028	8.124	0.967	3.063	3.265	5.407	6.194	6.868	6.974	8.918
	26 × 22	1.031	2.838	3.714	5.981	6.209	6.950	6.994	8.099	0.967	3.063	3.265	5.407	6.194	6.868	6.974	8.917
1	20 × 12	0.860	1.324	2.796	2.963	4.085	4.926	5.223	5.693	0.920	1.459	3.148	3.206	4.148	5.329	5.399	6.225
	24 × 20	0.859	1.324	2.793	2.955	4.084	4.924	5.199	5.678	0.920	1.459	3.148	3.206	4.148	5.329	5.399	6.225
	26 × 22	0.859	1.324	2.793	2.949	4.083	4.924	5.191	5.678	0.920	1.459	3.148	3.206	4.148	5.329	5.399	6.225
2	9 × 4	0.976	2.035	3.013	3.362	4.663	5.436	5.472	6.026	1.045	2.244	3.379	3.444	4.765	5.360	5.918	6.502
	20 × 12	0.969	2.034	2.988	3.259	4.621	5.185	5.398	5.727	1.038	2.243	3.376	3.425	4.750	5.309	5.870	6.255
	24 × 20	0.968	2.034	2.985	3.247	4.616	5.166	5.392	5.720	1.038	2.243	3.375	3.425	4.750	5.309	5.870	6.255
	26 × 22	0.968	2.034	2.985	3.241	4.612	5.158	5.391	5.720	1.038	2.243	3.375	3.425	4.750	5.309	5.870	6.255
3	9 × 4	1.412	2.532	3.677	3.808	5.370	5.617	5.880	6.031	1.494	2.794	3.882	4.059	5.373	5.657	6.303	6.528
	20 × 12	1.398	2.530	3.647	3.694	5.258	5.352	5.745	5.765	1.489	2.793	3.860	4.056	5.328	5.627	6.243	6.285
	24 × 20	1.396	2.530	3.645	3.681	5.238	5.343	5.738	5.750	1.489	2.793	3.860	4.056	5.327	5.627	6.242	6.285
	26 × 22	1.396	2.530	3.645	3.675	5.224	5.342	5.739	5.749	1.489	2.793	3.860	4.056	5.327	5.627	6.242	6.285

Table 5  
Convergence of the first eight eigenfrequency parameters for the free–clamped annular BaTiO<sub>3</sub>/CoFe<sub>2</sub>O<sub>4</sub> plates

<i>s</i>	<i>I</i> × <i>J</i>	BaTiO <sub>3</sub>								CoFe <sub>2</sub> O <sub>4</sub>							
		Ω <sub>1</sub>	Ω <sub>2</sub>	Ω <sub>3</sub>	Ω <sub>4</sub>	Ω <sub>5</sub>	Ω <sub>6</sub>	Ω <sub>7</sub>	Ω <sub>8</sub>	Ω <sub>1</sub>	Ω <sub>2</sub>	Ω <sub>3</sub>	Ω <sub>4</sub>	Ω <sub>5</sub>	Ω <sub>6</sub>	Ω <sub>7</sub>	Ω <sub>8</sub>
0	9 × 4	1.472	3.460	4.089	6.185	6.471	7.028	7.199	8.487	1.403	3.590	3.890	5.785	6.732	7.151	7.227	9.437
	24 × 20	1.405	3.449	3.806	5.968	6.067	6.769	7.060	8.251	1.387	3.563	3.880	5.702	6.428	7.081	7.114	9.185
	26 × 22	1.403	3.449	3.781	5.944	6.049	6.749	7.021	8.245	1.387	3.563	3.880	5.702	6.428	7.081	7.113	9.185
1	20 × 12	1.581	2.629	3.449	3.629	4.799	5.508	5.518	6.082	1.651	2.977	3.610	4.011	4.969	5.678	6.029	6.719
	24 × 20	1.578	2.628	3.433	3.628	4.797	5.498	5.515	6.077	1.651	2.977	3.610	4.011	4.968	5.678	6.029	6.719
	26 × 22	1.577	2.628	3.430	3.628	4.796	5.496	5.515	6.077	1.651	2.977	3.610	4.011	4.968	5.678	6.029	6.719
2	9 × 4	2.244	2.856	3.832	4.259	5.426	5.816	6.032	6.610	2.296	3.257	3.926	4.680	5.429	6.039	6.467	7.167
	20 × 12	2.208	2.843	3.727	4.254	5.213	5.725	5.860	6.365	2.275	3.248	3.906	4.679	5.360	6.019	6.384	6.962
	24 × 20	2.201	2.841	3.712	4.253	5.204	5.715	5.855	6.336	2.275	3.248	3.906	4.679	5.359	6.019	6.384	6.961
	26 × 22	2.199	2.840	3.708	4.253	5.199	5.714	5.855	6.336	2.275	3.248	3.906	4.679	5.359	6.019	6.384	6.961
3	9 × 4	3.032	3.343	4.400	5.069	5.794	6.368	6.418	6.978	3.069	3.759	4.533	5.547	5.744	6.780	6.826	7.550
	20 × 12	2.967	3.330	4.302	5.042	5.539	6.164	6.342	6.650	3.038	3.752	4.504	5.536	5.679	6.742	6.771	7.255
	24 × 20	2.952	3.329	4.288	5.040	5.519	6.154	6.333	6.627	3.038	3.752	4.504	5.536	5.678	6.742	6.771	7.255
	26 × 22	2.948	3.328	4.285	5.039	5.515	6.153	6.331	6.626	3.038	3.752	4.504	5.536	5.678	6.742	6.771	7.255

convergence of the free vibration frequencies for CoFe<sub>2</sub>O<sub>4</sub> plate is faster than BaTiO<sub>3</sub> plate. The same case happens in the other examples. This shows that the convergence of free vibration frequency of the magneto-elastic/electro-elastic annular plates is related to the corresponding materials.

Based on the above convergence study, the magneto-elastic/electro-elastic thin annular plates with inner radius  $R_0$  and outer radius  $R_1$  as well as thickness  $h$  ( $R_1/R_0 = 2$ ,  $h/R_1 = 0.01$ ) are also studied. Chebyshev polynomial terms are taken as  $I = K = N = O = Q = 25$ ,  $J = L = N = P = H = 20$ . The non-dimensional free vibration frequencies for wave number  $s = 0, 1, 2, 3$  for thin plates of BaTiO<sub>3</sub> and CoFe<sub>2</sub>O<sub>4</sub>, i.e.  $\Omega = \sqrt{\bar{\Omega}/C_{44}}$ , with different boundary conditions are listed in Table 6. The corresponding vibration modes



















Table 6

The first eight eigenfrequency parameters of each vibration category for the thin annular BaTiO<sub>3</sub>/CoFe<sub>2</sub>O<sub>4</sub> plates with different inner–outer boundary conditions (three distinct boundary conditions C–C, C–F and F–C in which the first capital letter denotes the inner boundary, while the second refer to outer boundary, and C means clamped, F means free)

BC	S	BaTiO <sub>3</sub>								CoFe <sub>2</sub> O <sub>4</sub>							
		$\Omega_1$	$\Omega_2$	$\Omega_3$	$\Omega_4$	$\Omega_5$	$\Omega_6$	$\Omega_7$	$\Omega_8$	$\Omega_1$	$\Omega_2$	$\Omega_3$	$\Omega_4$	$\Omega_5$	$\Omega_6$	$\Omega_7$	$\Omega_8$
C–C	0	0.395	1.046	2.387	3.771	6.012	6.377	7.846	9.879	0.256	0.702	1.369	2.244	3.321	4.587	6.032	6.364
	1	0.230	0.633	1.230	2.056	2.987	3.423	4.186	5.484	0.259	0.706	1.373	2.249	3.325	3.772	4.592	6.037
	2	0.238	0.644	1.242	2.069	3.000	3.875	4.199	5.437	0.267	0.718	1.386	2.263	3.339	4.306	4.606	6.051
C–F	0	0.396	1.032	2.054	3.144	3.403	5.031	6.480	9.223	0.244	0.696	1.363	2.241	3.209	3.321	4.594	6.047
	1	0.220	0.620	1.214	1.330	2.004	2.760	2.987	4.125	0.249	0.700	1.368	1.464	2.246	3.175	3.326	4.599
	2	0.234	0.633	1.227	1.938	2.018	2.839	3.000	4.139	0.263	0.715	1.383	2.134	2.261	3.238	3.341	4.613
F–C	0	0.405	0.939	1.659	2.980	3.334	4.943	6.017	8.826	0.267	0.718	1.385	2.263	3.343	3.556	4.615	6.068
	1	0.245	0.641	1.237	2.010	2.448	2.977	3.249	4.125	0.277	0.725	1.391	2.269	2.746	3.349	3.617	4.621
	2	0.270	0.662	1.255	2.028	2.678	2.994	3.679	4.140	0.303	0.748	1.412	2.288	3.065	3.367	4.049	4.638
	3	0.308	0.695	1.286	2.057	2.955	3.022	4.166	4.392	0.346	0.784	1.446	2.320	3.355	3.398	4.668	4.875

Table 7

Mode shapes of clamped–clamped annular BaTiO<sub>3</sub> plate

Mode number	Fundamental frequency	Mode shape			
		$U$	$\hat{v}$	$W$	$\Phi$
0	0.3953				
1	0.2301				
2	0.2383				
3	0.2530				

are shown in Tables 7–12 for middle plane  $z = 0$ . One can find that the vibration modes  $W$  and  $\Phi$  ( $\psi$ ) for BaTiO<sub>3</sub> (CoFe<sub>2</sub>O<sub>4</sub>) plate are somewhat similar each other. For BaTiO<sub>3</sub> plate, there is no vibration mode  $\psi$ , while for CoFe<sub>2</sub>O<sub>4</sub> plate there exists no vibration mode  $\Phi$ .

Similar to the isotropic annular plate, the fundamental non-dimensional eigenfrequency data  $\Omega = \sqrt{\Omega/C_{44}}$  for each of the vibration categories ( $s = 0, 1, 2, 3$ ) of magneto-elastic/electro-elastic thin annular plates with the clamped inner boundary and free outer boundary are obtained using the present method. Five different outer–inner radius ratios  $R_1/R_0 = 10, 10/2, 10/3, 10/7$  and  $10/9$  are analyzed. In calculation process,

Table 8  
Mode shapes of clamped–free annular BaTiO<sub>3</sub> plate

Mode number	Fundamental frequency	Mode shape			
		$U$	$\hat{v}$	$W$	$\Phi$
0	0.3965				
1	0.2195				
2	0.2342				
3	0.2534				

Table 9  
Mode shapes of free–clamped annular BaTiO<sub>3</sub> plate

Mode number	Fundamental frequency	Mode shape			
		$U$	$\hat{v}$	$W$	$\Phi$
0	0.4053				
1	0.2452				
2	0.2697				
3	0.3080				

Chebyshev polynomial terms are chosen to be  $I = K = N = O = Q = 25$ ,  $J = L = N = P = H = 20$ . The fundamental eigenfrequencies of each vibration category with respect to the thickness–radius  $t/R_1$  are shown in Figs. 1–8, respectively. From Figs. 1 and 2, one can find that for the given value  $R_1/R_0$  the fundamental non-dimensional eigenfrequency of axisymmetric vibration  $s = 0$  reaches to almost constant value with the increase of the thickness–radius  $t/R_1$ , and for the given value of  $t/R_1$ , the fundamental non-dimensional axisymmetric vibration eigenfrequency increases with the decrease of the outer–inner radius ratios  $R_1/R_0$ .

Table 10  
Mode shapes of clamped–clamped annular CoFe<sub>2</sub>O<sub>4</sub> plate




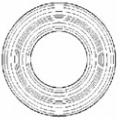









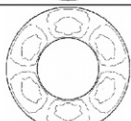
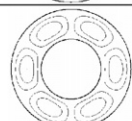
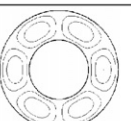





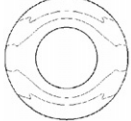
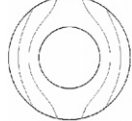
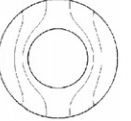

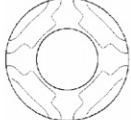
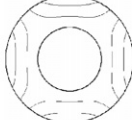
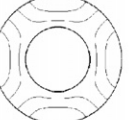




Mode number	Fundamental frequency	Mode shape			
		$U$	$\hat{v}$	$W$	$\Psi$
0	0.2557				
1	0.2585				
2	0.2673				
3	0.2832				

Table 11  
Mode shapes of clamped–free annular CoFe<sub>2</sub>O<sub>4</sub> plate

Mode number	Fundamental frequency	Mode shape			
		$U$	$\hat{v}$	$W$	$\Psi$
0	0.2443				
1	0.2488				
2	0.2626				
3	0.2857				

Similar case can also be observed from Figs. 3 and 4 for the circumferential vibration  $s = 1$ . From Figs. 5 and 6, one can observe that two eigenfrequency curves for  $R_1/R_0 = 10/2, 10/3$  are almost the same for various values of  $t/R_1$ , while with the increase of inner radius of annular plate the fundamental non-dimensional eigenfrequency of circumferential vibration  $s = 2$  increases and reaches to certain constant value with the increase of various values of  $t/R_1$ . Figs. 7 and 8 show that for different outer–inner radius ratios, only when  $R_1/R_0 = 10/9$  the fundamental non-dimensional eigenfrequency of circumferential vibration  $s = 3$  fast reaches to one constant value with the increase of various values of  $t/R_1$ .

Table 12  
Mode shapes of free-clamped annular  $\text{CoFe}_2\text{O}_4$  plate

Mode number	Fundamental frequency	Mode shape			
		$U$	$\hat{v}$	$W$	$\Psi$
0	0.2443				
1	0.2488				
2	0.2626				
3	0.2857				

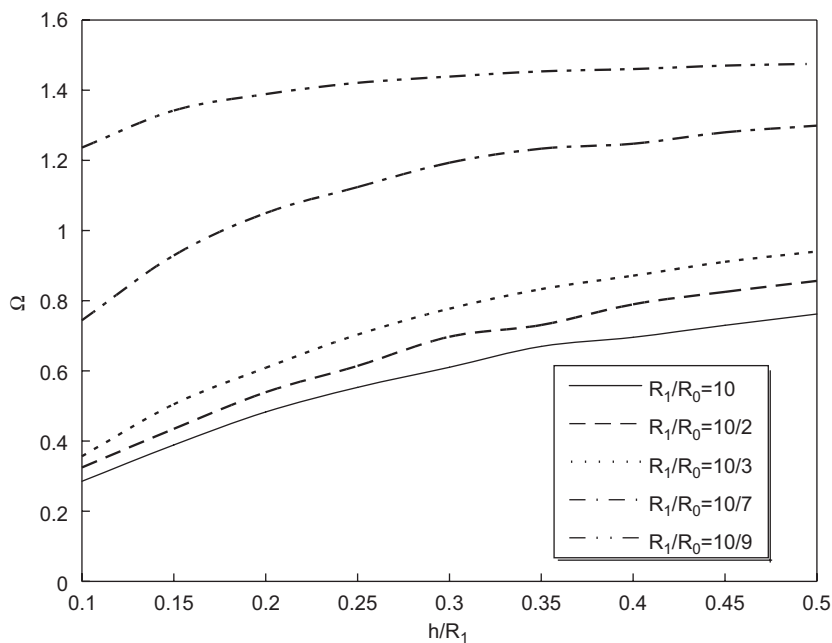


Fig. 1. The fundamental eigenfrequencies of axisymmetric vibration ( $s = 0$ ) for  $\text{BaTiO}_3$  annular plates with clamped inner boundary and free outer boundary.

#### 4. Conclusions

In this paper, 3D free vibration analysis of magneto-elastic/electro-elastic circular/annular plates have been studied using the Chebyshev–Ritz method which has been successfully used to carry out free vibration analysis of various isotropic plates (e.g. Refs. [10–12]). The convergence rate of magneto-elastic/electro-elastic circular/annular plates with different boundary conditions has been shown by using various Chebyshev polynomial

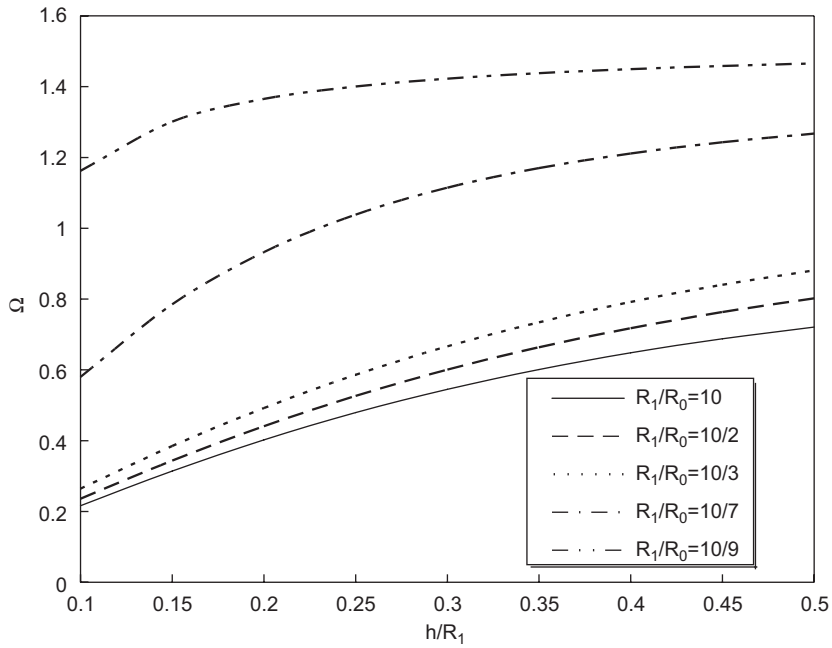


Fig. 2. The fundamental eigenfrequencies of axisymmetric vibration ( $s = 0$ ) for  $\text{CoFe}_2\text{O}_4$  annular plates with clamped inner boundary and free outer boundary.

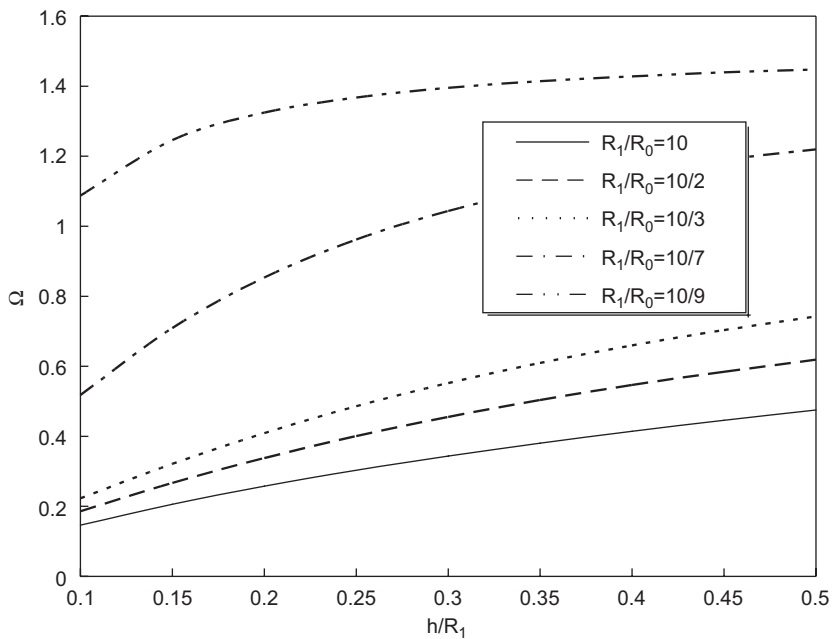


Fig. 3. The fundamental eigenfrequencies of circumferential vibration ( $s = 1$ ) for  $\text{BaTiO}_3$  annular plates with clamped inner boundary and free outer boundary.

terms. Besides, the effect of geometrical parameters and material properties of the problems on the free vibration eigenfrequencies has been considered. The obtained results can be used to check the accuracy of other numerical methods, i.e. finite element method and boundary element method.

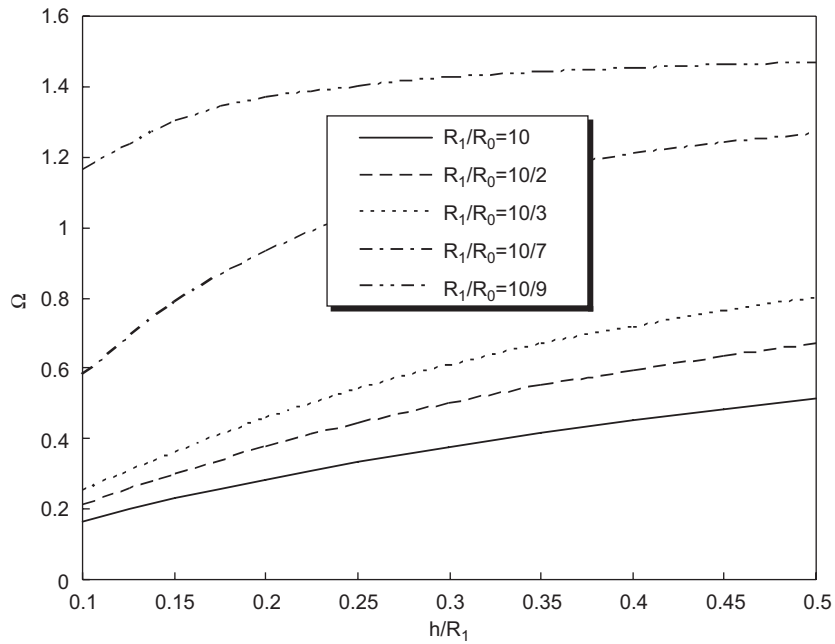


Fig. 4. The fundamental eigenfrequencies of circumferential vibration ( $s = 1$ ) for  $\text{CoFe}_2\text{O}_4$  annular plates with clamped inner boundary and free outer boundary.

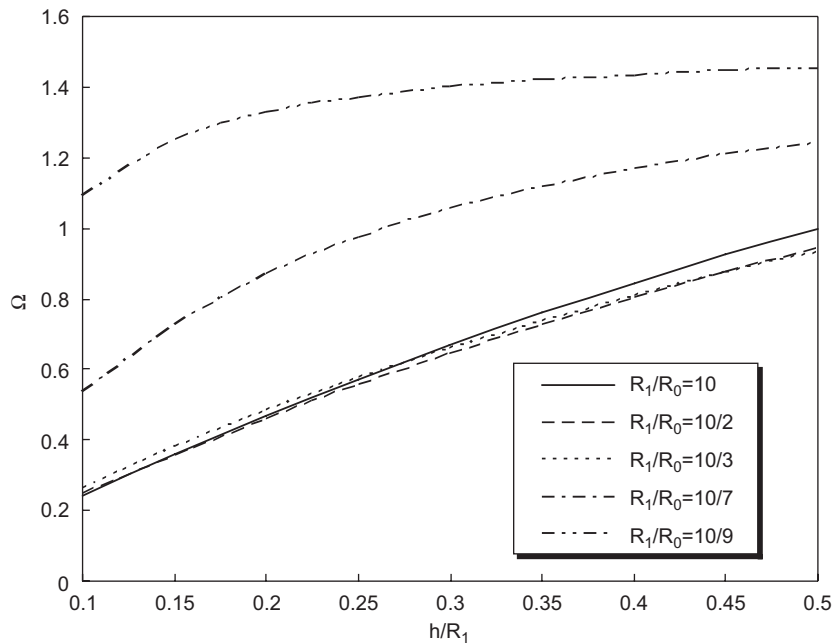


Fig. 5. The fundamental eigenfrequencies of circumferential vibration ( $s = 2$ ) for  $\text{BaTiO}_3$  annular plates with clamped inner boundary and free outer boundary.

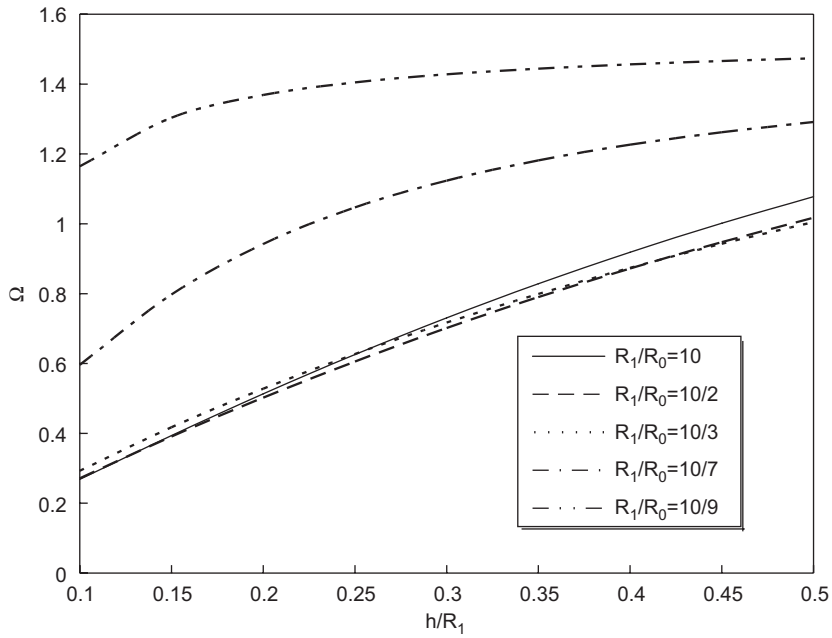


Fig. 6. The fundamental eigenfrequencies of circumferential vibration ( $s = 2$ ) for  $\text{CoFe}_2\text{O}_4$  annular plates with clamped inner boundary and free outer boundary.

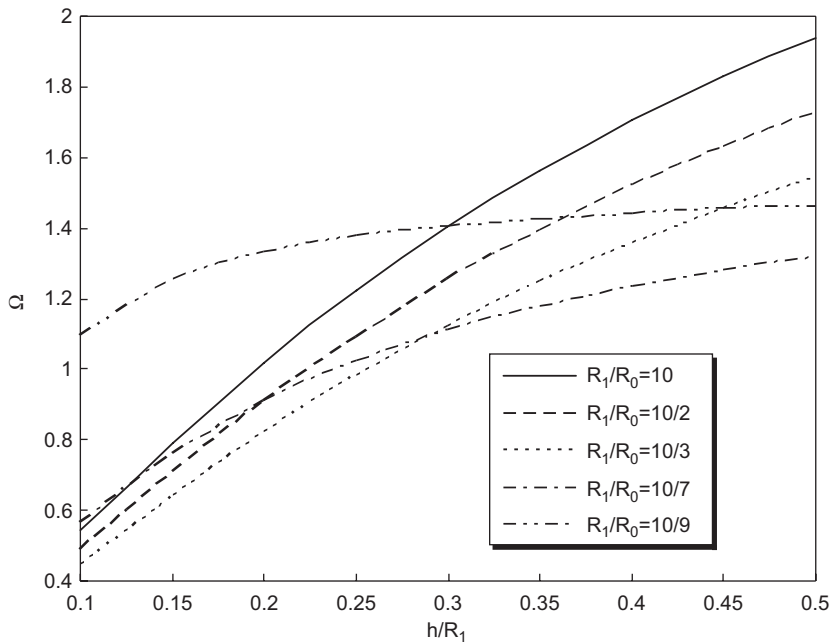


Fig. 7. The fundamental eigenfrequencies of circumferential vibration ( $s = 3$ ) for  $\text{BaTiO}_3$  annular plates with clamped inner boundary and free outer boundary.

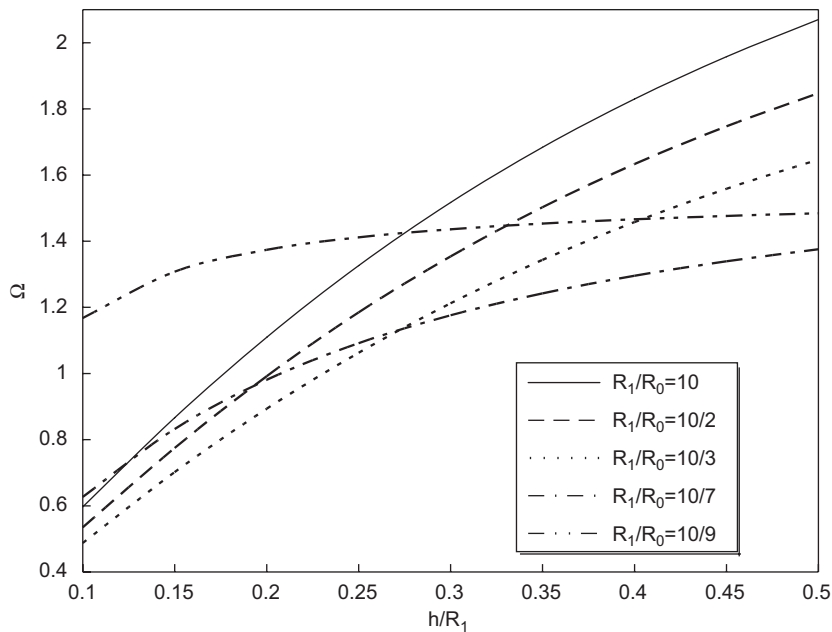


Fig. 8. The fundamental eigenfrequencies of circumferential vibration ( $s = 3$ ) for  $\text{CoFe}_2\text{O}_4$  annular plates with clamped inner boundary and free outer boundary.

## Acknowledgments

This work was supported by the National Natural Science Foundation of China under Grant no. 10772030. The authors would like to thank two anonymous reviewers for their constructive comments and suggestions on this paper.

## References

- [1] H.J. Ding, A.M. Jiang, A boundary integral formulation and solution for 2D problems in magneto-electro-elastic media, *Computers and Structures* 82 (2004) 1599–1607.
- [2] E. Pan, Exact solution for simply supported and multilayered magneto-electro-elastic plates, *Transactions of the ASME* 68 (2001) 608–618.
- [3] E. Pan, P.R. Heyliger, Free vibrations of simply supported and multilayered magneto-electro-elastic plates, *Journal of Sound and Vibration* 252 (3) (2002) 429–442.
- [4] X. Wang, Z. Zhong, A finitely long circular cylindrical shell of piezoelectric/piezomagnetic composite under pressuring and temperature change, *International Journal of Engineering Science* 41 (2003) 2429–2445.
- [5] W.Q. Chen, K.Y. Lee, Alternative state space formulations for magneto electric thermo elasticity with transverse isotropy and the application to bending analysis of nonhomogeneous plate, *International Journal of Solids and Structures* 40 (2003) 5689–5705.
- [6] W.Q. Chen, K.Y. Lee, H.J. Ding, On free vibration of non-homogeneous transversely isotropic magneto-electro-elastic plates, *Journal of Sound and Vibration* 279 (2005) 237–251.
- [7] G.R. Buchanan, Free vibration of an infinite magneto-electro-elastic cylinder, *Journal of Sound and Vibration* 268 (2003) 413–426.
- [8] R.K. Bhangale, N. Ganesan, Free vibration studies of simply supported non-homogeneous functionally graded magneto-electro-elastic finite cylindrical shells, *Journal of Sound and Vibration* 288 (2005) 412–422.
- [9] A.R. Annigeri, N. Ganesan, S. Swarnamani, Free vibrations of clamped-clamped magneto-electro-elastic cylindrical shells, *Journal of Sound and Vibration* 292 (2006) 300–314.
- [10] D. Zhou, Y.K. Cheung, F.T.K. Au, S.H. Lo, Three-dimensional vibration analysis of thick, rectangular plates using Chebyshev polynomial and Ritz method, *International Journal of Solids and Structures* 39 (2002) 6339–6353.
- [11] D. Zhou, F.T.K. Au, Y.K. Cheung, S.H. Lo, Three-dimensional vibration analysis of circular and annular plates via the Chebyshev–Ritz method, *International Journal of Solids and Structures* 40 (2003) 3089–3105.



- [12] D. Zhou, S.H. Lo, F.T.K. Au, Y.K. Cheung, W.Q. Liu, 3-D vibration analysis of skew thick plates using Chebyshev–Ritz method, *International Journal of Mechanical Sciences* 48 (2006) 1481–1493.
- [13] W.H. Press, B.P. Flannery, S.A. Teukolsky, W.T. Vetterling, *Numerical Recipes—The Art of Scientific Computing*, Cambridge University Press, Cambridge, 1986.
- [14] Y. Wang, R.Q. Xu, H.J. Ding, Free vibration of piezoelectric annular plate, *Journal of Zhejiang University Science* 4 (2003) 379–387.